Staggered versus overlap fermions: A study in the Schwinger model with $N_f=0,1,2$

Stephan Dürr
DESY Zeuthen, Platanenallee 6, D-15738 Zeuthen, Germany

Christian Hoelbling
Centre de Physique Théorique, Case 907, CNRS Luminy, F-13288 Marseille Cedex 9, France
(Received 10 November 2003; published 24 February 2004)

We study the scalar condensate and the topological susceptibility for a continuous range of quark masses in the Schwinger model with $N_f=0,1,2$ dynamical flavors, using both the overlap and the staggered discretization. At finite lattice spacing the differences between the two formulations become rather dramatic near the chiral limit, but they get severely reduced, at the coupling considered, after a few smearing steps.

DOI: 10.1103/PhysRevD.69.034503 PACS number(s): 11.15.Ha, 11.10.Kk

I. INTRODUCTION

Recently, the staggered action when coupled to HYP-smeared backgrounds [1] has attracted renewed interest. This is mainly due to the cheapness of this formulation which bears the promise that realistic unquenched simulations can be performed with currently available resources [2]. Moreover, as a remnant of the full $SU(N_f=d)_A$ group, the continuous "two-hop global" symmetry

$$\chi(x)\to\exp[i\theta_A(-1)^{\Sigma n_\nu}]\chi(x),$$
$$\overline{\chi}(x)\to\overline{\chi}(x)\exp[-i\theta_A(-1)^{\Sigma n_\nu}], \tag{1}$$

where $x=a(n_1,\ldots,n_d)$ protects the fermion mass against additive renormalization. On the other hand, taking the square and quartic root of the determinant (to obtain $N_f=2+1$ dynamical flavors) might spoil the locality of the action [3], and the often believed insensitivity to topology could undermine attempts to push towards the chiral limit.

The other extreme in terms of computational cost is represented by the closely related domain-wall [4] and overlap [5] fermions. For these actions, the Ginsparg-Wilson relation [6]

$$D\hat{\gamma}_5+\gamma_5 D=0,\quad \hat{\gamma}_5=\gamma_5\left(1-\frac{a}{\rho}D\right) \tag{2}$$

holds in the massless limit [with ρ for the moment an arbitrary parameter that will be specified in Eq. (5)], implying invariance under the full chiral symmetry group [7]

$$\delta\psi=\hat{\gamma}_5\psi,\quad \delta\overline{\psi}=\overline{\psi}\gamma_5 \tag{3}$$

at finite lattice spacing, which again excludes additive mass renormalization and prevents operators in different chiral multiplets from mixing.

Given this situation, we decided to investigate the difference between staggered and overlap fermions at finite lattice spacing in a simple theory where the concept of chiral symmetry proves relevant and some interesting quantities are known analytically. These criteria are fulfilled by the generalized Schwinger model (QED in 2D with N_f massive degenerate fermions), a super-renormalizable theory [8] where the scale is set through the dimensionful fundamental coupling

$$g=\frac{1}{a\sqrt{\beta}}. \tag{4}$$

We produced 10 000 independent gauge configurations on a $N\times N=20^2$ lattice with the standard (compact) Wilson gauge action at $\beta=4$, giving a plaquette of 0.86279(10). For each configuration we determine the complete eigenvalue spectrum of the massless overlap and staggered operators. This allows us to compute—for any given mass—the condensate and the fermion determinant, which we use to reweight our observables to $N_f=1,2$ [9].

We define the massive overlap operator as

$$D_m^{\rm ov}=\left(1-\frac{am}{2\rho}\right)D^{\rm ov}+m,\quad aD^{\rm ov}=1+\gamma_5\,\mathrm{sign}(a\gamma_5 D_{-\rho}^{\rm W}) \tag{5}$$

with $D_{-\rho}^{\rm W}$ the Wilson operator at negative mass $-\rho/a$. We further set $\rho=1$, which we checked, following Ref. [10], is an almost optimal choice with respect to locality at our coupling.

Previous work on the Schwinger model using a direct approach for the computation of the scalar condensate is collected in Refs. [11–13] for staggered, domain wall/overlap or both actions, respectively. We checked that we reproduce the staggered condensate from Ref. [13] and the overlap condensate of FHLW/GHR in Ref. [12].

II. SCALAR CONDENSATE

In the chiral limit, the $N_f=1$ scalar condensate is given by [8]

$$\frac{\chi_{\rm sca}(m=0)}{g}=\frac{e^\gamma}{2\pi^{3/2}}=0.1599\cdots\quad [N_f=1]. \tag{6}$$

For $N_f=2$ a nonzero value would signal spontaneous symmetry breaking and therefore violate the Mermin-Wagner-

Hohenberg-Coleman theorem [14]. The prediction how explicit symmetry breaking modifies this zero is [15]

$$\frac{\chi_{\rm sca}}{g}=0.388\cdots\left(\frac{m}{g}\right)^{1/3}\qquad [N_f=2]. \tag{7}$$

In the staggered formulation we follow Ref. [11] and implement the (1-flavor) condensate through

$$\frac{\chi_{\rm sca}}{g}=-\frac{1}{2}\frac{1}{N^2 g}\langle\overline{\chi}\chi\rangle, \tag{8}$$

where the purpose of the factor 1/2 is to compensate the two-fold degeneracy of the staggered formulation in 2D. Denoting the eigenvalues of the massless staggered Dirac operator by λ (they show up in complex conjugate pairs with zero real part), the reweighted condensate is

$$\frac{\chi_{\rm sca}}{g}=\frac{1}{2}\frac{1}{L^2 g}\frac{\left\langle \det(D_m^{\rm st})^{N_f/2}\sum\frac{1}{(\lambda+m)}\right\rangle}{\langle\det(D_m^{\rm st})^{N_f/2}\rangle},$$

$$\det(D_m^{\rm st})=\prod\,(\lambda+m). \tag{9}$$

with $L=Na$ and the sum and product running over the entire spectrum. In Ref. [11] one finds also the associated free field limit

$$\frac{\chi_{\rm sca}}{g}=\frac{2}{N^2}\frac{m}{g}\sum_{i,j=1}^{N/2}\frac{1}{(am)^2+\sin(2\pi i/N)^2+\sin(2\pi j/N)^2} \tag{10}$$

which is, of course, independent of N_f.

For overlap fermions, the scalar condensate is unambiguously defined as [12]

$$\frac{\chi_{\rm sca}}{g}=-\frac{1}{N^2 g}\langle\overline{\psi}\hat{\psi}\rangle,\qquad \hat{\psi}=\frac{1+\gamma_5\hat{\gamma}_5}{2}\psi. \tag{11}$$

Denoting the eigenvalues of the massless overlap Dirac operator by λ, and remembering that we work with $\rho=1$, the reweighted condensate is

$$\frac{\chi_{\rm sca}}{g}=\frac{1}{L^2 g}\frac{\left\langle \det(D_m^{\rm ov})^{N_f}\sum\frac{1-a\lambda/2}{(1-am/2)\lambda+m}\right\rangle}{\langle\det(D_m^{\rm ov})^{N_f}\rangle},$$

$$\det(D_m^{\rm ov})=\prod\left[\left(1-\frac{am}{2}\right)\lambda+m\right], \tag{12}$$

where the sum runs over the full spectrum. These eigenvalues occur either in complex conjugate pairs or as isolated chiral (doubler) modes at $a\lambda=0(2)$. Finally, one can rewrite Eq. (12) as

$$\frac{\chi_{\rm sca}}{g}=\frac{1}{L^2 g}\frac{\left\langle \det(D_m^{\rm ov})^{N_f}\sum{}'\frac{1}{\hat{\lambda}+m}\right\rangle}{\langle\det(D_m^{\rm ov})^{N_f}\rangle},\quad \hat{\lambda}=\left(\lambda^{-1}-\frac{a}{2}\right)^{-1}, \tag{13}$$

where $a\hat{\lambda}$ is purely imaginary and the sum excludes the doubler modes at $a\lambda=2$.

Due to the (remnant) chiral symmetry of (staggered) overlap fermions, no subtraction of the condensate at zero quark mass is required. Furthermore, the Schwinger model is super-renormalizable, i.e., there is no renormalization needed at infinite cutoff. In fact, due to the dimensionful coupling (4), all lattice renormalization factors have the form $Z=1+O(a^2g^2)$ and therefore are 1, up to $O(a^2)$ corrections. Hence, both the staggered and the overlap discretization yield (for any N_f and $m>0$) a finite condensate which is subject to $O(a^2)$ cutoff effects with unit Z-factor plus an additive piece proportional to m.

A modification which is motivated by what is done in full QCD simulations, is to consider the Dirac operator on a "copy" of an element of the Markov chain on which one applies one or more APE/HYP smearing steps (which in 2D is the same). One then thinks of the operator as one in the original links, which is less local. For the staggered action, such a modification preserves the universality class while considerably reducing the "taste" violation [16]. Being unaware of any detailed understanding of what the optimum smearing parameter is, we decided to combine the staple and the original link with equal weight, which means in a $U(1)$ theory that one takes the arithmetic mean of the phases.

Figure 1 displays our results for the scalar condensate. As expected, the overlap condensate exhibits the qualitatively correct behavior in the chiral limit. For $N_f=0$ it shows the quenched divergence, while for $N_f=2$ it tends to zero indicating the absence of spontaneous chiral symmetry breaking. In the $N_f=1$ case it tends to a constant which seems compatible with the analytic result (6) in infinite volume, marked by an asterisk. Here, we dare to compare to the infinite volume value, since the results in Ref. [17] suggest that for $N_f=1$ in a box with $L>1/(\sqrt{\pi}g)$ finite volume corrections are exponentially small. On the other hand, the staggered condensate exhibits a *qualitatively wrong* behavior in the chiral limit, vanishing for all N_f. At large masses it differs substantially from the overlap condensate, presumably due to cutoff effects. In the intermediate region, there is a smooth turnover with no sign of a quenched divergence.

The dashed curve is Smilga's infinite volume result (7), while the dash-dotted graph represents the free-field expression (10). Finally, since changing m at fixed box-volume V means that one moves from the large to the small Leutwyler-Smilga regime, the point where the Leutwyler-Smilga parameter [18]

$$x=V\Sigma m \tag{14}$$

equals 1 is indicated with a vertical dotted line [Σ denotes the analytical result (6)].

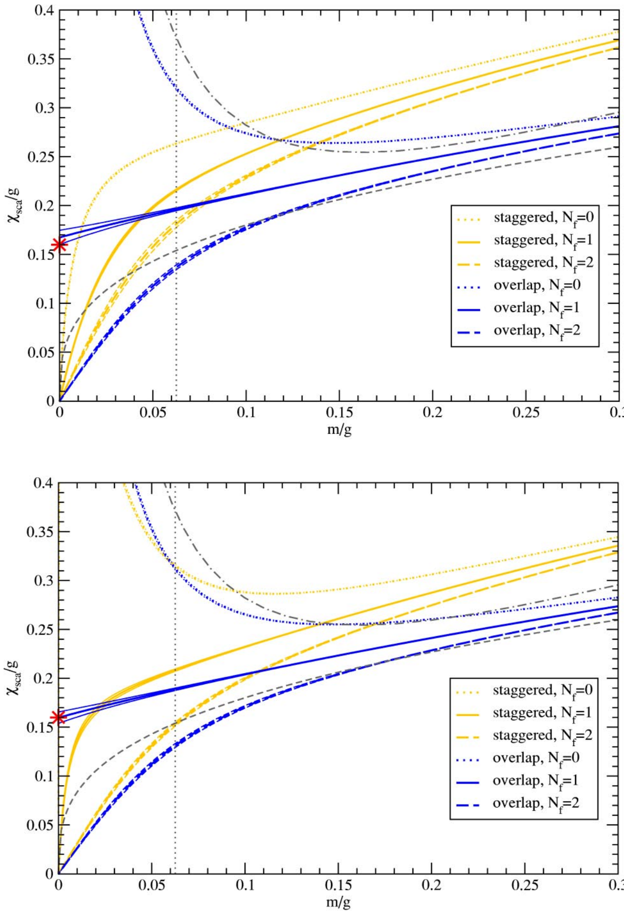

FIG. 1. Scalar condensate after 0 (top) and 1 (bottom) steps of APE/HYP smearing.

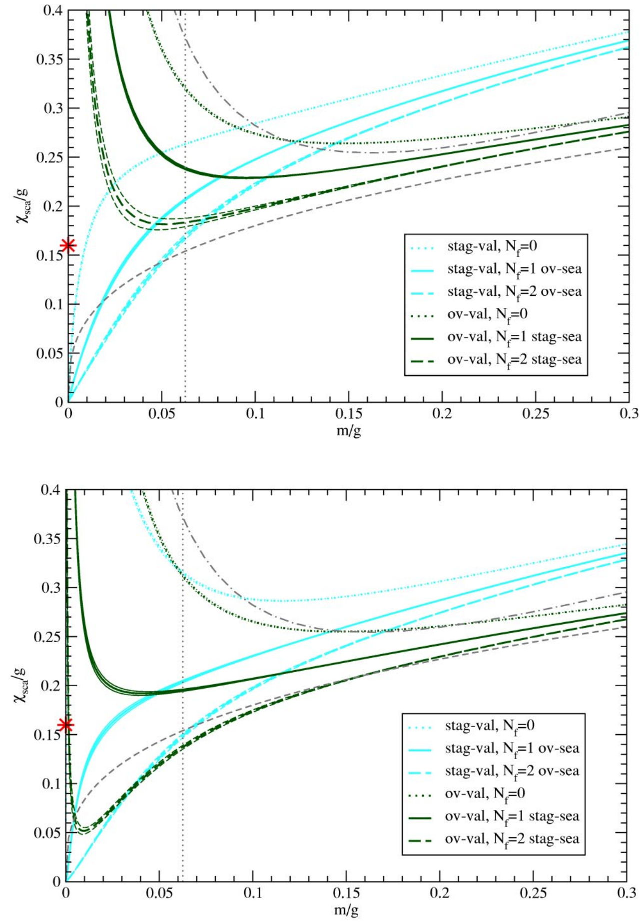

FIG. 2. Hybrid condensate after 0 (top) and 1 (bottom) steps of APE/HYP smearing.

The real surprise comes when the operators are evaluated after one step of APE/HYP smearing. The overlap condensate stays (for any N_f) virtually unchanged, except that the size of the $O(a^2)$ artefacts is modified. Formally, the same statement holds true with the staggered action, but from a quantitative point of view the change is rather dramatic. In the $N_f=1$ case one can ''trust'' it down to much smaller quark masses, until it finally collapses. And for $N_f=0$ it shows a nice blow-up at moderately small quark masses. If one really considers the limit $m \to 0$ it still tends to zero, but the point where this happens is deep within the ϵ regime ($x \ll 1$) [18]. The effect of additional smearing steps will be discussed below.

Figure 2 shows our results for the ''hybrid'' condensate, labeled after the formulation used for the valence quark. The ''staggered'' condensate (with $N_f=1,2$ sea quarks built from the overlap determinant) looks virtually unchanged with respect to Fig. 1 (the curve with $N_f=0$ is identical). On the other hand, the ''overlap'' condensate (with $N_f=1,2$ sea quarks constructed from the staggered determinant) looks much worse than the original (true) overlap version; there is a divergence near $m=0$ for any N_f. This shows that the failure of the unsmeared (''naive/thin-link'') staggered formulation cannot be attributed to either the determinant or the valence prescription alone—it is the cancellation of the zero in the determinant and the ''one over zero'' in the propagator which is needed to get the finite value (6) in the 1-flavor case.

Upon applying just one step of smearing the situation improves dramatically; both ''hybrids'' look qualitatively right down to much smaller quark masses—but still, eventually the nonfaithful representation of the zero mode(s) in the staggered part reflects itself in a fake blow-up or drop-down close to the chiral limit.

Figure 3 contains our results for the condensate in a log-log representation. The overlap data show that the analytic structure in a finite volume is indeed

$$\chi_{\rm scal} \propto \begin{cases} 1/m & (N_f=0), \\ \text{const} & (N_f=1), \\ m & (N_f=2) \end{cases} \tag{15}$$

near the chiral limit and consistent with

$$\chi_{\rm scal} \propto m^{1/3} \tag{16}$$

at large masses, albeit the coefficient in Eq. (7) is (presumably due to cutoff effects) not reproduced.

The bottom part demonstrates that 3 APE/HYP-smearing steps manage to completely change the overall picture of the

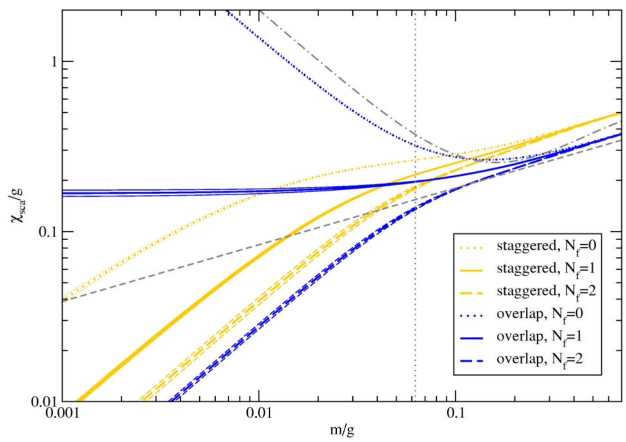

FIG. 3. Scalar condensate after 0 (top) and 3 (bottom) steps of APE/HYP smearing.

staggered condensate while the overlap condensate gets rescaled by a factor which differs from 1 only marginally. Now, the two formulations are in perfect agreement at (moderately) small quark masses, showing only a mild discrepancy at larger m/g: the staggered condensate seems to tend towards the free-field limit (10), while the overlap version moves closer to Smilga's prediction (7). Eventually, the staggered condensate vanishes in the chiral limit—even for $N_f=0$. The turnover point, however, is off the scale of the plot.

III. SELECTION THEOREM

A remarkable feature of the Schwinger model with $N_f=1$ is the "selection theorem." This theorem states that in the chiral limit the nonzero value (6) is formed *exclusively* from the zero modes of chirality ± 1, which live on backgrounds where the topological charge

$$q(A)=\frac{g}{4\pi}\int \epsilon_{\mu\nu}F_{\mu\nu}dx\in \mathbf{Z} \tag{17}$$

takes the value ∓ 1. This statement alludes to a combination of the Atiyah-Singer index theorem and the vanishing theorem. The former relates Eq. (17) to the index of the Dirac operator, defined as the difference of the number of negative and positive chirality zero modes

$$\mathrm{ind}(A)=n_- - n_+ \tag{18}$$

in a simple manner

$$q(A)=\mathrm{ind}(A), \tag{19}$$

while the latter says that in 2D there is no configuration which supports both positive and negative chirality zero modes [19]

$$n_-\neq 0 \Rightarrow n_+=0,$$
$$n_+\neq 0 \Rightarrow n_-=0. \tag{20}$$

To prove the "selection theorem" one starts from the partition function of the massless theory in the finite volume with periodic boundary conditions ($N_f \geqslant 1$) [17]

$$Z[\bar{\eta},\eta]=N\sum_{q\in \mathbf{Z}}\int DA^{(q)}e^{-(1/4)\int F^2} \times\left(\prod_{k=1}^{|q|}(\bar{\eta}\psi_k)(\bar{\psi}_k\eta)\right)^{N_f}\det{}'(D)^{N_f}e^{+\int\bar{\eta}S'\eta} \tag{21}$$

from which the condensate is computed by taking *one* derivative with respect to $\bar{\eta}$ and η and then setting the external sources to zero. The outer sum is over all topological sectors and the product is over the $|q|$ positive *or* negative chirality zero modes. The primes indicate that the determinant and the fermion Green's function are computed on the subspace orthogonal to the zero modes. A nonzero value is obtained *only* if both derivatives hit the prefactor, leaving nothing but the explicit zero mode and its conjugate behind. This can happen only for $N_f=1$ and results in a condensate which is generated *exclusively* by the zero modes with chirality ± 1. Note that the argument will hold true in QCD, too, once the current body of numerical evidence in favor of a vanishing theorem in 4D (see Fig. 1 in Ref. [20]) has been replaced by a mathematical proof.

As a technical point we mention that on the lattice we define the topological charge of a background U as the index of the massless overlap operator [21,7]

$$q(U)=\mathrm{ind}(U)=\tfrac{1}{2}\mathrm{tr}(a\gamma_5 D^{\mathrm{ov}}) \tag{22}$$

and use it for both the staggered and the overlap evaluation of the sectoral condensate.

Figure 4 displays our results for the condensate if we truncate the partition function at a given $|q|_{\max}$. The overlap construct faithfully reproduces the "selection theorem," which means that the $N_f=1$ condensate tends to zero if one restricts it to the topologically trivial sector, while it takes the Schwinger value (6) in the chiral limit for any other $|q|_{\max}$.

Analogously, the staggered condensate exhibits (for both N_f shown) a many-sigma difference between $|q|_{\max}=0,1,2$. This disproves the widely believed fiction that staggered fermions are "insensitive to topology"—but they are *not sen-*

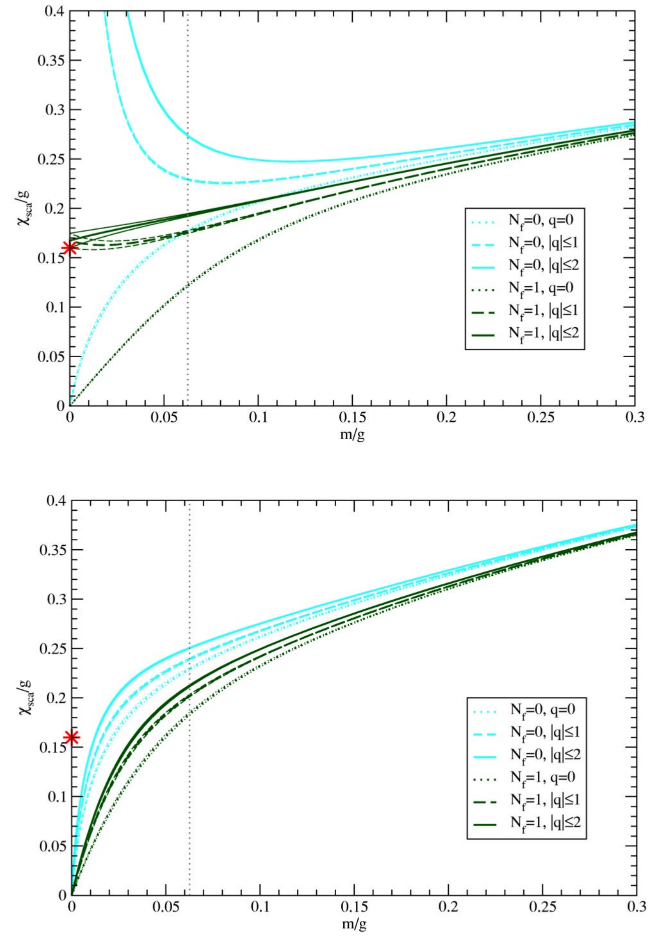

FIG. 4. Sectoral condensate for overlap (top) and staggered quarks without smearing.

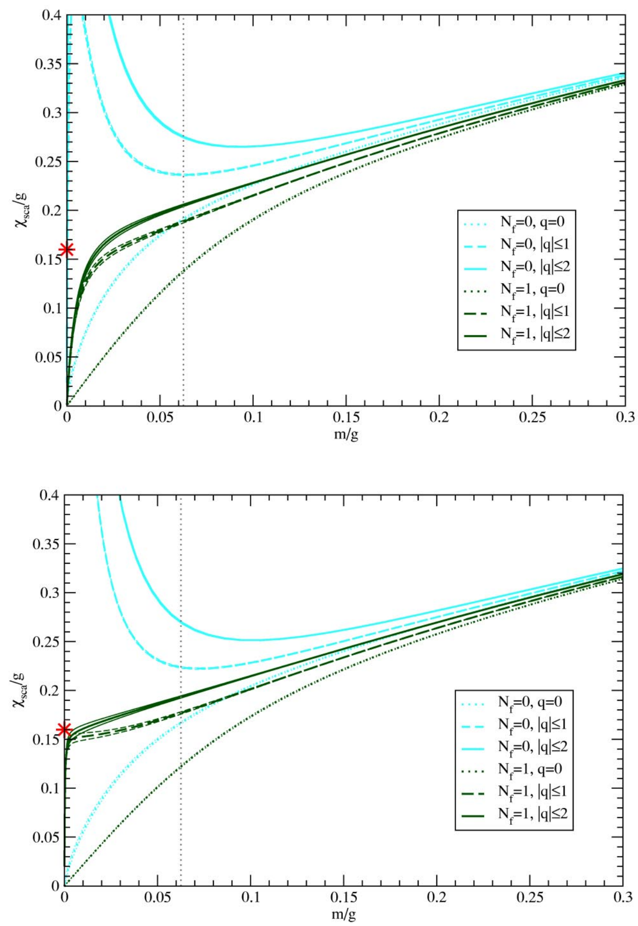

FIG. 5. Sectoral condensate for staggered quarks with 1 and 3 steps of APE/HYP smearing.

sitive the right way; they do not seem to know about the index and the vanishing theorems which are at the root of the ‘‘selection theorem.’’

Figure 5 shows that the real surprise comes again after one or a few APE/HYP-smearing steps. Already one step lets the staggered $N_f=1$ condensate (at intermediate mass) develop a marked sensitivity on the topological charge of the background.

After two more steps the qualitative picture is just as in the (unsmeared) overlap case (see Fig. 4), i.e., smeared staggered fermions do know about the relationship between topology and the chirality of zero modes—down to rather small (but nonzero) quark masses. Of course, if one really performs the chiral limit, the staggered condensate still tends to zero—for any $|q|_{\max}$ and even in the quenched case $(N_f=0)$. This is visible in the top of Fig. 5, while in the bottom part it is off the scale.

Since in the Schwinger model various observables have been seen to depend on the topological charge [22], it is surprising that the ‘‘selection theorem’’ has not been checked before.

IV. TOPOLOGICAL SUSCEPTIBILITY

Another interesting observable to study the effects of dynamical fermions is the topological susceptibility which, in the context of this note, shall be *defined* (in the continuum) through

$$\chi_{\mathrm{top}}=\lim_{V\to\infty}\frac{\langle \det(D+m)^{N_f}q^2\rangle}{V\langle \det(D+m)^{N_f}\rangle}. \tag{23}$$

The main difference to the scalar condensate is that the topological susceptibility depends only on the *sea* quarks, thus offering a potentially cleaner view at the effects of square-rooting the staggered determinant to get $N_f=1$.

For staggered quarks, the definition (23), taken in fixed volume, reduces to

$$\frac{\chi_{\mathrm{top}}}{g^2}=\frac{\beta}{N^2}\,\frac{\langle \det(D_m^{\mathrm{st}})^{N_f/2}q^2\rangle}{\langle \det(D_m^{\mathrm{st}})^{N_f/2}\rangle}, \tag{24}$$

while for overlap quarks, the implementation reads

$$\frac{\chi_{\mathrm{top}}}{g^2}=\frac{\beta}{N^2}\,\frac{\langle \det(D_m^{\mathrm{ov}})^{N_f}q^2\rangle}{\langle \det(D_m^{\mathrm{ov}})^{N_f}\rangle}, \tag{25}$$

where $\det(D_m^{\mathrm{st}})$ and $\det(D_m^{\mathrm{ov}})$ are defined in Eqs. (9), (12). In either case the sum is over the spectrum of the massless

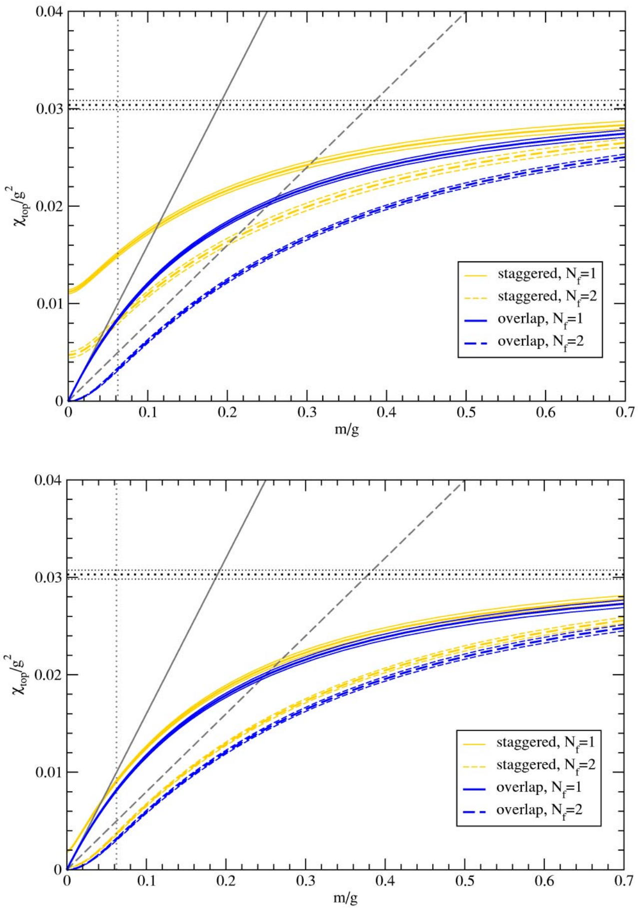

FIG. 6. Topological susceptibility with 0 (top) and 1 steps of APE/HYP smearing.

operator, and we apply the overlap definition (22) of the topological charge in both Eqs. (24) and (25).

Finally we would like to mention the continuum prediction how the topological susceptibility in QCD tends to zero, if the quark mass does [18] [the LS parameter x was defined in Eq. (14)],

$$\chi_{\rm top} = \frac{\Sigma m}{N_f} \quad (N_f = 1 \vee x \gg 1), \tag{26}$$

$$\chi_{\rm top} \propto m^{N_f} \quad (x \ll 1). \tag{27}$$

Figure 6 contains our results for the mass dependence of the topological susceptibility, defined via Eqs. (24), (25). The full and the dashed lines represent the prediction of Eq. (26) for the cases $N_f = 1,2$, respectively. One can see that for both discretizations $\chi_{\rm top}$ gets suppressed by dynamical fermion effects, but close to the chiral limit only the overlap determinant leads to results which are compatible with the QCD prediction (26) for $N_f = 1$ and (27) for $N_f = 2$.

Again, just one smearing step proves sufficient to almost eliminate the lattice artefacts the "unsmeared/naive" staggered determinant was plagued with, while the topological susceptibility for overlap fermions stays basically invariant under such a modification.

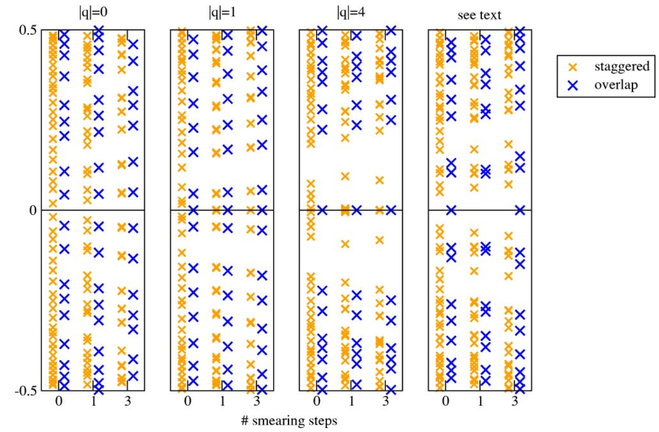

FIG. 7. Physically relevant region of the Dirac spectrum on some selected configurations.

V. SPECTRAL HINT

As a hint of what is the likely reason behind the remarkable success of one or a few APE/HYP smearing steps at the β value considered, we would like to present the effect of such a modification on the spectrum of some individual configurations. In Fig. 7 we plot the physically relevant part of the spectrum of the staggered [the $a\lambda$ from Eq. (9)] and overlap [the $a\hat{\lambda}$ from Eq. (13)] operator on four selected configurations before and after smearing.

The two configurations on the left are typical examples for topological charge $q = 0$ and $|q| = 1$, respectively. One sees that on the unsmeared configurations the staggered spectrum does not resemble that of the overlap operator. Furthermore, it is hard to see a qualitative difference between $q = 0$ and $|q| = 1$ in the spectrum of the original staggered operator. After a few smearing steps this picture changes. The eigenvalues of the staggered operator seem to form near-degenerate pairs which sit close to a single overlap $a\hat{\lambda}$ on the same configuration. In particular, in the $|q| = 1$ case a pair of eigenmodes moves very close to the real axis. Clearly, such a shift mimics the effect of the true zero mode in the overlap counterpart down to rather small quark masses. It is only when the mass becomes comparable to the smallest (smeared staggered) eigenvalue that the absence of an exact zero-mode matters and a qualitative difference between the staggered and overlap Dirac operators (on that configuration) shows up.

In the third column of Fig. 7, a typical configuration with higher topological charge ($|q| = 4$) is displayed. Here, the picture is not so nice any more, since after 3 smearing steps only 3 pairs of eigenmodes have come close to the real axis and the fourth one is still somewhat further out.

To show that these findings are not generic, the last column of Fig. 7 presents a selected configuration on which the topological charge varies repeatedly under subsequent smearing steps. Qualitative resemblance between the spectra of the two operators is vague at best and there is no evidence of a pair of staggered eigenvalues moving close to the real axis. Obviously, such "sick" configurations will occur more frequently at larger coupling.

VI. SUMMARY

Our findings may be summarized by the following statements:

(1) At finite spacing and in a finite box, the ''naive'' staggered action leads to a scalar condensate which is *qualitatively wrong*: the staggered results vanish in the chiral limit for any N_f, while the overlap successfully reproduces the quenched $\sim 1/m$ divergence, and the analytically known Schwinger value in the chiral limit for $N_f=1$.

(2) Considering both types of ''hybrid'' formulations (staggered valence quarks with overlap sea quarks and vice versa) we find that the failure of the naive staggered formulation cannot be attributed to either the determinant or the propagator alone.

(3) The ''selection theorem'' is reproduced, in an impressive manner, with overlap fermions, while naive staggered fermions fail completely.

(4) The topological susceptibility shows lattice artefacts which are large for unimproved staggered fermions, while the overlap results seem consistent with the known chiral behavior.

(5) Taking the square root of the staggered determinant to have $N_f=1$ seems to be no more or less harmful than dividing by 2, in the valence sector, to get the 1-flavor condensate. All naive staggered results seem to only gradually vary for $N_f=0,1,2$—even near the chiral limit, where they should not.

(6) At the β value considered, already one smearing step brings a remarkable improvement: although formally the chiral limit of staggered fermions is still wrong, the mass at which one begins to see this is dramatically lowered. At moderate quark masses, one observes a clear blow up of the APE/HYP smeared staggered condensate for $N_f=0$, while it stays close to the Schwinger value (6) for $N_f=1$ and keeps the qualitatively correct behavior at $N_f=2$. Moreover, in spite of naive staggered fermions being misguided in the way they see topology, the APE/HYP variety condensate shows a remarkable sensitivity on $|q|_{\max}$ for $N_f=0$ and $N_f=1$, reproducing the ''selection theorem'' in the latter case. Finally, the staggered artefacts in the topological susceptibility get drastically reduced, resulting in good agreement with the overlap curve down to very small quark masses.

(7) The main difference after a few smearing steps is the size of lattice artefacts in the condensate at large quark masses which make the smeared overlap condensate (for any N_f) lie closer to the analytical prediction (7) by Smilga, while the smeared staggered values move more towards the free field prediction (10). The qualitative failure of staggered fermions in the chiral limit is only visible at very small quark masses.

(8) Under moderate smearing the modes of the massless staggered Dirac operator form near-degenerate pairs which move close to the corresponding overlap (single) eigenvalues $(\hat{\lambda})$, supporting the square root and factor 1/2 procedure for staggered spectroscopy. On nontrivial backgrounds the mismatch between the staggered fake zero mode and the true overlap zero gives an estimate of the quark mass at which the deficiency of the staggered formulation gets visible, though there are configurations which break this analogy.

As a warning against an overly optimistic interpretation of 6/8, we feel obliged to recall that we were working with fairly smooth gauge fields. It is not clear whether such a nice pattern holds true also in QCD at accessible couplings.

ACKNOWLEDGMENTS

We are indebted to Gunnar Bali for bringing to our attention the interest in checking chiral properties of staggered fermions in a simple model. We thank Steve Sharpe for the suggestion to study the effect of APE/HYP smearing. S.D. wishes to acknowledge useful discussions with Rainer Sommer, C.H. with Christian Lang and Laurent Lellouch. S.D. is supported by DFG in SFB/TR-9, C.H. is supported by EU Grant No. HPMF-CT-2001-01468.

[1] A. Hasenfratz and F. Knechtli, Phys. Rev. D **64**, 034504 (2001).

[2] HPQCD Collaboration, C. T. Davies *et al.*, Phys. Rev. Lett. **92**, 022001 (2004).

[3] K. Jansen, hep-lat/0311039.

[4] D.B. Kaplan, Phys. Lett. B **288**, 342 (1992); Y. Shamir, Nucl. Phys. **B406**, 90 (1993).

[5] R. Narayanan and H. Neuberger, Nucl. Phys. **B412**, 574 (1994); **B443**, 305 (1995); H. Neuberger, Phys. Lett. B **417**, 141 (1998); **427**, 353 (1998).

[6] P.H. Ginsparg and K.G. Wilson, Phys. Rev. D **25**, 2649 (1982).

[7] M. Lüscher, Phys. Lett. B **428**, 342 (1998).

[8] J.S. Schwinger, Phys. Rev. **128**, 2425 (1962).

[9] C.B. Lang and T.K. Pany, Nucl. Phys. **B513**, 645 (1998).

[10] P. Hernandez, K. Jansen, and M. Lüscher, Nucl. Phys. **B552**, 363 (1999).

[11] E. Marinari, G. Parisi, and C. Rebbi, Nucl. Phys. **B190**, 734 (1981); J. Polonyi and H.W. Wyld, Phys. Rev. Lett. **51**, 2257 (1983); **52**, 401(E) (1984); T. Burkitt, Nucl. Phys. **B220**, 401 (1983); A.N. Burkitt and R.D. Kenway, Phys. Lett. **131B**, 429 (1983); S.R. Carson and R.D. Kenway, Ann. Phys. (N.Y.) **166**, 364 (1986); M. Grady, Phys. Rev. D **35**, 1961 (1987).

[12] R. Narayanan, H. Neuberger, and P. Vranas, Nucl. Phys. B (Proc. Suppl.) **47**, 596 (1996); Phys. Lett. B **353**, 507 (1995); F. Farchioni, I. Hip, and C.B. Lang, *ibid.* **443**, 214 (1998); F. Farchioni, I. Hip, C.B. Lang, and M. Wohlgenannt, Nucl. Phys. **B549**, 364 (1999); J.E. Kiskis and R. Narayanan, Phys. Rev. D **62**, 054501 (2000); L. Giusti, C. Hoelbling, and C. Rebbi, *ibid.* **64**, 054501 (2001).

[13] S. Chandrasekharan, Phys. Rev. D **59**, 094502 (1999).

[14] N.D. Mermin and H. Wagner, Phys. Rev. Lett. **17**, 1133 (1966); P.C. Hohenberg, Phys. Rev. **158**, 383 (1967); S.R. Coleman, Commun. Math. Phys. **31**, 259 (1973).

[15] A.V. Smilga, Phys. Rev. D **55**, 443 (1997).

[16] T. Blum *et al.*, Phys. Rev. D **55**, 1133 (1997).

[17] I. Sachs and A. Wipf, Helv. Phys. Acta **65**, 652 (1992).
[18] H. Leutwyler and A. Smilga, Phys. Rev. D **46**, 5607 (1992).
[19] J.E. Kiskis, Phys. Rev. D **15**, 2329 (1977); N.K. Nielsen and B. Schroer, Nucl. Phys. **B127**, 493 (1977); M.M. Ansourian, Phys. Lett. **70B**, 301 (1977).
[20] T. Blum *et al.*, Phys. Rev. D **65**, 014504 (2002).
[21] P. Hasenfratz, V. Laliena, and F. Niedermayer, Phys. Lett. B **427**, 125 (1998).
[22] H. Dilger and H. Joos, Nucl. Phys. B (Proc. Suppl.) **34**, 195 (1994); S. Dürr, Nucl. Phys. **B594**, 420 (2001); Nucl. Phys. B (Proc. Suppl.) **106**, 598 (2002); H. Fukaya and T. Onogi, Phys. Rev. D **68**, 074503 (2003).